Journal of Fluids and Structures 17 (2003) 1095–1110

JOURNAL OF FLUIDS AND STRUCTURES

www.elsevier.nl/locate/jnlabr/yjfls

Model study of noise field in the human chest due to turbulent flow in a larger blood vessel

A.O. Borisyuk*

Institute of Hydromechanics, Zhelyabova Street 8/4, 03680 Kiev-180 MSP, Ukraine

Received 16 October 2000; accepted 31 March 2003

Abstract

An acoustic generation of noise by a larger human blood vessel and noise transmission in the thorax is modelled and studied. In making this, the random statistical nature of the noise sources, the basic vessel properties and the main features of the human chest structure are taken into account. Also the effects of changes in the basic vessel parameters are considered as a first approach to study acoustic effects of a vascular stenosis. The analysis of the resultant acoustic field reveals its similarity to the acoustic fields recorded in the appropriate experiments. The variations in the basic vessel parameters are found to cause the corresponding changes in the sound level and the production of new frequency components in the acoustic power spectrum. The acoustic power from a slightly thickened vessel is shown to be approximately proportional to the fourth power of the flow Reynolds number in the originally normal vessel and the eighth power of the ratio of the vessel diameters.

1. Introduction

The *noninvasive* acoustic diagnosis of stenotic obstructions of vessels is of a great concern to the medical clinician. It uses the noise field induced in vessel and perceived at the skin surface as sounds (Duncan et al., 1975; Lees and Dewey, 1970; Mirolyubov, 1983; Young, 1979). The essential measurements are the spectral and correlation characteristics of the sound field from which information about stenosis (such as the presence, location, shape, characteristic dimensions, etc.) can be obtained. However, the *quantitative* diagnosis of a stenosis is only possible if the fundamental mechanisms of vascular sound generation and transmission are known. There exist a number of studies (Borisyuk, 1998, 1999, 2000; Duncan et al., 1975; Fredberg, 1974, 1977; Lees and Dewey, 1970; Mirolyubov, 1983; Young, 1979), which suggest that the most probable sources of sounds associated with blood motion are turbulent pressure fluctuations in the flow.

With the sources known, an acoustic model of an appropriate vascular district of the human blood passages can be developed. Such a model must correctly describe the rheological properties of blood and the nature of the flow in the vessel, the physical and geometrical characteristics of the vessel, a stenotic obstruction, the structure and physical properties of the human body, etc. As a result, it must correctly describe the acoustic generation and transmission of noise from the source to the receiver resting on the skin and, therefore, correctly predict the relationships between the characteristics of the source and the recorded signal which is necessary for solving the *inverse* problem (viz. locating pathology by changes in the characteristics of the noise field picked up periodically from the chest surface of a given patient).

Analysis of the scientific literature shows that the creation of an acoustic model of a separate blood vessel is still far from complete. To the author's knowledge, at present only a few works (Borisyuk, 1998, 1999; Vovk et al., 1994a, b;

*Corresponding author. Semashko Street 21, 88, 03142 Kiev 142, Ukraine. Tel.: +380-44-450-5110; fax: +380-44-455-6432.
E-mail address: oibor@nas.gov.ua (A.O. Borisyuk).

0889-9746/03/$ - see front matter
doi:10.1016/S0889-9746(03)00056-2

Nomenclature

a	radius of pipe midsurface
$a_n(\omega)$	response term for the nth normal mode of pipe
$\lvert A_{vn}(k_z)\rvert^2$	shape functions
c	sound speed in fluid
c_0	sound speed in acoustic medium
c_v	longitudinal wave speed in pipe wall
d	inner diameter of thickened pipe
D	inner diameter of conditionally normal pipe
D_v	bending stiffness of pipe wall
E_v	Young's modulus of pipe wall
f	frequency
h	thickness of pipe wall
H	height of cylinder and length of pipe
Δh	thickening of pipe wall
k_0	acoustic wavenumber
k_{0m}	wavenumber of the mth acoustic mode
k_{vn}	wavenumber of the nth normal mode of pipe
k_z	wavenumber in the flow direction
$P(\omega)$	power spectrum of turbulent wall pressure
p_0	acoustic pressure
p_t	turbulent wall pressure
$P_w(r, z, \omega)$	spectral density of radial acceleration in acoustic wave
R	radius of cylinder
Re_D	Reynolds number of mean flow in normal pipe
r, z	radial and axial coordinates, respectively
S	severity of pipe narrowing
t	time
u	mean flow velocity in thickened pipe
U	mean flow velocity in normal pipe
U_c	convective velocity in normal pipe
v_*	friction velocity
w_r	radial acceleration in acoustic wave
Z_{0m}	acoustic modes

Greek letters

α_{0m}	radial wavenumber
μ_0	damping coefficient in acoustic medium
ν	kinematic viscosity of fluid
ν_v	Poisson's ratio of pipe wall
Π	acoustic power
ρ	mass density of fluid
ρ_0	mass density of acoustic medium
ρ_v	mass density of pipe wall
$\Phi_p(k_z, \omega)$	wavenumber–frequency spectrum of turbulent wall pressure
$\Phi_{p_n}(\omega)$	excitation term for the nth normal mode of pipe
$\Phi_{p*}(k_z, \omega)$	wavenumber–frequency spectrum normalized to unity
$\Psi_{vn}(z)$	in vacuo normal modes of pipe
ω	circular frequency
ω_m	cut-off frequencies
ω_{vn}	in vacuo natural frequencies of pipe

Wang et al., 1990; Wodicka et al., 1989, 1990) can be reported in which the *simplest* such models are introduced, some of them being the models of a larger airway of the human respiratory system (Vovk et al., 1994a, b; Wodicka et al., 1989, 1990). (However, these models can be easily adapted to the case of a larger blood vessel for the corresponding parameter values.) Although undoubtedly important, these works have, however, significant disadvantages, namely, in the model suggested by Wodicka et al. (1989, 1990) the source of sound is given by an infinite circular cylinder with an inner determined loading, and the body is introduced as an infinite homogeneous medium of known density, sound speed and damping coefficient. The disadvantages of such an approach are that it does not take into account either the finiteness of the vessel and the human thorax or the random statistical nature of fluid loading, as well as the vessel elasticity.

A few years later Vovk et al. (1994a) have outlined a simple qualitative model which looked much similar to that developed by Wodicka et al. (1989, 1990).

In the more recent paper by Vovk et al. (1994b), two finite coaxial circular cylinders, with random turbulent pressures at the surface of the inner cylinder, were considered. This is a more realistic approach compared with the one above. However, here the authors have not considered both the presence of a stenotic obstruction and the elastic properties of the vessel wall. A vessel was treated as the massless fluid–body tissue interface. In addition, they have used the Corcos model (Corcos, 1963) for turbulent wall pressure fluctuations, the disadvantages of which are well known (Borisyuk, 1993; Borisyuk and Grinchenko, 1997; Martin and Leehey, 1977).

Wang et al. (1990) have made an attempt to describe a vascular stenosis. Their model consisted of two finite, isolated elastic cylinders, joined in series and excited by inner random turbulent forces. One cylinder simulated an arterial stenosis, and the other was a post-stenotic segment of an artery. In general, such an approach looks interesting. However, it requires some clarifications and completions to be made. Namely, the difference in the wall bending stiffness of the stenosed and normal segments of the vessel should be taken into account. Also both the boundary conditions for the cylinders and the turbulent wall pressure field, as well as the influence of the body tissue on the sound field need to be described more adequately.

A model developed by Borisyuk (1998, 1999) has taken account of the above-mentioned basic features of the acoustic generation and transmission of noise in the human chest from the source to the receiver, and permitted consideration of a simple stenotic narrowing in the vessel. The acoustic power spectra produced by conditionally normal and narrowed pipes were studied, and some characteristic signs of the presence of vessel constriction have been found.

The present work further develops this model by including mass and elasticity of the vessel wall, as well as by considering flow–structure interaction and more realistic boundary conditions. The paper consists of five sections and a list of references. The formulation of the problem and the appropriate assumptions are made in Section 2. The analytical solution for the acoustic field in the thorax is constructed in Section 3. Predictions for the acoustic field generated at some typical conditions and the analysis of the field are carried out in Section 4. Finally, the conclusions of the investigation are made in Section 5.

2. Formulation of the problem

Precise modelling of vascular sound generation and transmission in the body is difficult. However, noting that the characteristic scales and dimensions of the basic factors which specify these two mechanisms are small compared with the acoustic wavelengths of interest in vascular stenosis murmurs, it is possible to make simplifying assumptions. Under these assumptions, the basic elements of the simulated acoustic channel of noise generation and transmission can be described quite well within the accepted limits of accuracy. As a result, the spectral and correlation characteristics of noise field modelled will be similar to those recorded from patients.

Taking these arguments into account, we shall use the following considerations and assumptions in describing the constructive elements of the problem to be studied in this work.

Larger blood vessel. A finite elastic thin-walled pipe of circular cross-section is chosen to represent a larger human blood vessel. In such a pipe, only the basic vessel properties are reflected. These include mass and elasticity of the wall, small wall-thickness/diameter ratio, a finite length and proximity of the vessel shape to cylindrical. The more sophisticated details of the vessel geometry and wall mechanics (such as curvature, taper shape, wall tension, the layered structure of the wall, etc.) are neglected at this stage of the qualitative study of the acoustic field of vessel and the effects of variation in the basic vessel parameters. This is justified because these details will not have a great effect on the qualitative results of this work (which show us what changes in the acoustic field are caused by the above variations rather than how much these variations influence the field). Their inclusion will result in the quantitative changes in the vibration field (i.e., the amplitudes and resonance frequencies, etc.), and hence the acoustic field of the vessel (i.e., the

spectral levels and the position of the maxima at these frequencies, etc.). However, the quantitative effects are not the subject of this work.

Vessel abnormality. Appearance of a stenosis is associated with changes in many vessel parameters. The most important, from the acoustical point of view, are local reduction of the cross-sectional area of the vessel, increase in the bending stiffness and changes in the mass density of the vessel wall. These variations greatly influence the noise source structure within the artery, and hence the structure of the acoustic field in the body. In this paper, uniform changes (along the vessel axis) in these parameters are considered as a first step to study acoustic effects of a vascular stenosis.

Flow. The frequency range of interest in vascular stenosis murmurs is determined by the parameters of flow, vessel and stenosis, and usually lies between 20 Hz and 1 kHz (Borisyuk, 2000). This is high compared with the cardiac cycle frequencies (~ 1 Hz). Consequently, the average flow rate changes associated with the cardiac cycle represent a slow variation compared with the relevant disturbed flow fluctuations and associated acoustic field oscillations. As a first order of approximation, we therefore make the usual quasi-steady assumption that during the observation of the disturbed flow and acoustic field fluctuations the flow rate remains essentially unchanged, and consequently the fluctuations depend mainly on the instantaneous flow rate. This investigation therefore focuses on the quasi-steady flow problem with flow rate (or, at constant diameter of the pipe, mean axial flow velocity) as one of the physical parameters.

The next simplification is that the flow is assumed to be fully developed turbulent under any vessel conditions. This allows the use of existing low Mach number models for turbulent wall-pressure spectra which look similar to those formed by a localized constriction in the artery (Borisyuk, 1999, and references therein). Such a choice of the model for the fluid loading at the vessel surface will not have a great influence on the qualitative effects of variation in the basic vessel parameters, because (i) the difference between the fluid loadings in real blood flow and that considered here will be significantly smoothed out due to averaging in the statistical characteristics of noise fields calculated for those loadings; (ii) the difference between the noise fields produced by flow in the vessel before and after appearance of abnormality (this difference is one of the basic parameters to be analysed in diagnosing the vessel state) is less sensitive to the choice of fluid loading than the noise fields themselves.

Thorax. Since the thorax shape is close to cylindrical, and the characteristic dimensions of the thorax and the details of its geometry are small in terms of the acoustic wavelengths of interest in vascular stenosis murmurs, the thorax can be represented by a finite circular cylinder. Another assumption relates to the thorax tissue itself. The available data (Borisyuk, 2000, and references therein) indicate that the tissue can be considered in the first approximation as homogeneous acoustic medium with averaged properties. We therefore represent the tissue by such a medium, the choice of values for the medium parameters being made in accordance with that given by Wodicka et al. (1989, 1990) and Vovk et al. (1994a, b).

The above assumptions allow the formulation of the problem of noise generation by flow of blood into the human thorax. The geometry under consideration is depicted in Fig. 1a. Here the thorax is represented by a finite circular cylinder, of height H and radius R, filled with an acoustic medium of density ρ_0, sound speed c_0 and damping coefficient μ_0 and surrounded by air. The medium represents the body tissue. The vessel is simulated by a finite coaxial circular thin-walled elastic pipe, of length H, radius of midsurface a ($a/R \ll 1$) and wall thickness h ($h/a \ll 1$). The pipe wall has the modulus of elasticity E_v, mass density ρ_v and Poisson's ratio ν_v. The flow in the pipe is fully developed turbulent, and characterized by the mean axial velocity U. The fluid (blood) has mass density ρ, sound speed c and kinematic viscosity ν. The vessel is excited by turbulent wall pressure fluctuations and radiates sound into the thorax. The spectral characteristics of the sound heard at the chest surface can then be determined and analysed in order to diagnose the vessel state.

The formulated problem of finding the acoustic field between two finite coaxial cylinders, due to flow–pipe interaction, is axisymmetric (i.e., $\partial/\partial\phi = 0$), and governed by two coupled equations. These are the equation of the pipe motion written for the normal velocity $v(z,t)$ of the pipe wall, viz. (Junger and Feit, 1972)

$$D_v \frac{\partial^4 v}{\partial z^4} + \frac{E_v h}{a^2(1-\nu_v^2)} v + \rho_v h \frac{\partial^2 v}{\partial t^2} = \frac{\partial}{\partial t}(p_0|_{r=a} - p_t), \quad 0 < z < H, \tag{1}$$

and the two-dimensional wave equation describing sound radiation by the vibrating pipe, viz. (Borisyuk, 1998; Junger and Feit, 1972)

$$\nabla^2_{(r,z)} p_0 - \frac{1}{\bar{c}_0^2} \frac{\partial^2 p_0}{\partial t^2} = 0, \quad a < r < R, \ \ 0 < z < H, \tag{2}$$

$$\nabla^2_{(r,z)} = \frac{1}{r}\frac{\partial}{\partial r}\left(r \frac{\partial}{\partial r}\right) + \frac{\partial^2}{\partial z^2}, \quad \bar{c}_0 = c_0(1 + \mathrm{i}\mu_0).$$

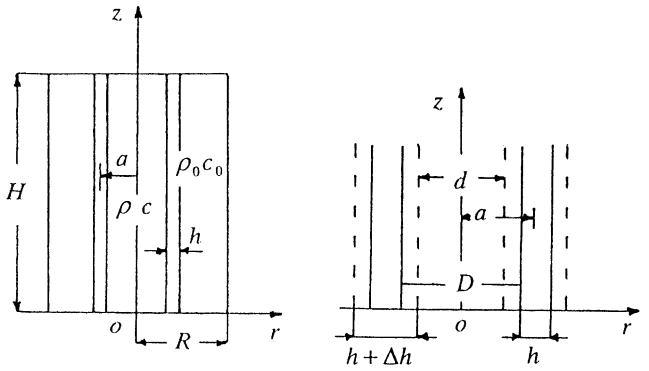

Fig. 1. (a) Geometry of the problem; (b) thickening of the pipe wall.

Here $p_t(z,t)$ and $p_0(r,z,t)$ are the turbulent pressure at the inner surface of the tube and the acoustic pressure generated by the forced motion of the tube, respectively, D_v the pipe bending stiffness, i$=\sqrt{-1}$ a complex unity, and the origin of the cylindrical coordinate system (r,ϕ,z) is taken in the centre of the cylinder bottoms. The random turbulent pressure field is assumed to be temporally stationary and spatially homogeneous, and D_v is related to the vessel Young's modulus E_v, thickness h, and Poisson's ratio v_v, by $D_v = E_v h^3/[12(1-v_v^2)]$.

Without loss of generality, the boundary conditions for the pipe can be taken as simply supported, viz. (Junger and Feit, 1972)

$$v|_{z=0,H} = 0, \quad \frac{\partial^2 v}{\partial z^2}|_{z=0,H} = 0. \tag{3}$$

Since the wave resistance of the thorax tissue, $\rho_0 c_0$, is much lower than that of the thorax bottom and much higher than that of air (Borisyuk, 1998, 1999; Vovk et al., 1994b), the lower side of the outer cylinder can be treated as acoustically rigid, and both the upper side and the lateral surface of this cylinder as pressure-released. Therefore, the boundary conditions for Eq. (2) are written as

$$\frac{\partial p_0}{\partial z}|_{z=0} = 0, \quad p_0|_{z=H} = p_0|_{r=R} = 0, \tag{4}$$

and the system of Eqs. (1)–(4) is completed by condition linking $p_0(r,z,t)$ and $v(z,t)$ at the pipe surface, viz.

$$-\frac{1}{\rho_0}\frac{\partial p_0}{\partial r}|_{r=a} = \frac{\partial v}{\partial t}. \tag{5}$$

As was said in the assumptions, the effects of uniform reduction of the cross-sectional area of the vessel, increase in the bending stiffness and changes in the mass density of the vessel wall are of interest in this study. Within the framework of the acoustic model under discussion these changes in the vessel state can be simulated by the appropriate variations in the geometrical and/or physical parameters of the pipe. Firstly, this is the thickening Δh of the pipe wall (Fig. 1b) resulting both in a mild reduction of the cross-sectional area of the pipe, viz.

$$\begin{aligned} &\textit{normal pipe}: \quad D = 2a - h, \\ &\textit{narrowed pipe}: \quad d = 2a - h - \Delta h, \quad (\Delta h/h)_{\max} \sim 1, \end{aligned} \tag{6}$$

and increase in the bending stiffness D_v. The mass conservation within the pipe before and after the appearance of the wall thickening is assumed in this case, viz.

$$UD^2 = ud^2, \tag{7}$$

and the mean axial flow velocity in the narrowed pipe, u, is therefore written as

$$u = U(D/d)^2 \approx U\left(1 + \frac{\Delta h}{2a}\right)^2. \tag{8}$$

Secondly, increase in the wall bending stiffness D_v can be caused by the increase in the Young's modulus E_v and/or Poisson's ratio v_v, and changes in the mass density of the vessel wall are obtained by the variation of the pipe parameter ρ_v itself.

3. Acoustic field between the cylinders

The solution to the problem (1)–(5) is obtained by taking the Fourier transform, defined here with the convention

$$g(k_z,\omega)=\frac{1}{(2\pi)^2}\int_{-H/2}^{H/2}\int_{-\infty}^{\infty} g(z,t)\mathrm{e}^{-\mathrm{i}(k_z z-\omega t)}\,\mathrm{d}z\,\mathrm{d}t, \tag{9}$$

and performing a modal analysis. The in vacuo normal modes $\Psi_{vn}(z)$ of the simply supported pipe satisfy the equation

$$D_v\frac{d^4\Psi_{vn}}{dz^4}-(\rho_v h\omega_{vn}^2-\frac{E_v h}{a^2(1-v_v^2)})\Psi_{vn}=0, \tag{10}$$

and the boundary conditions (3) and are given by the expression

$$\Psi_{vn}(z)=\sin(k_{vn}z),\quad n=1,2,\ldots \tag{11}$$

with modal wavenumbers $k_{vn}=n\pi/H$ and in vacuo natural frequencies of flexural vibrations of the pipe:

$$\omega_{vn}=\frac{c_v}{a}\sqrt{1+(k_{vn}a)^4\frac{h^2}{12a^2}}, \tag{12}$$

in which $c_v=\sqrt{E_v/\rho_v(1-v_v^2)}$ is the longitudinal wave speed in the pipe wall.

The modal equations are found by writing the velocity in Eq. (1) as an infinite sum of individual mode components,

$$v(z,\omega)=\frac{1}{2\pi}\int_{-\infty}^{\infty} v(z,t)\mathrm{e}^{\mathrm{i}\omega t}\,\mathrm{d}t=\sum_{n=1}^{\infty} V_n(\omega)\Psi_{vn}(z) \tag{13}$$

and using the orthogonality properties of the normal modes, viz.

$$\int_0^H \Psi_{vn}(z)\Psi_{vm}(z)\,\mathrm{d}z=\begin{cases}H/2 & \text{for } m=n,\\ 0 & \text{for } m\neq n.\end{cases}$$

This process yields

$$\rho_v h(\omega_{vn}^2-\omega^2)V_n(\omega)=-\mathrm{i}\omega[p_{0n}(\omega)-p_{tn}(\omega)], \tag{14}$$

where $p_{0n}(\omega)$ and $p_{tn}(\omega)$ are of similar form and defined by

$$p_{0n}(\omega)=\frac{2}{H}\int_0^H p_0(r=a,z,\omega)\Psi_{vn}(z)\,\mathrm{d}z,$$

$$p_{tn}(\omega)=\frac{2}{H}\int_0^H p_t(z,\omega)\Psi_{vn}(z)\,\mathrm{d}z. \tag{15}$$

The acoustic pressure $p_0(r,z,\omega)$ can be written as

$$p_0(r,z,\omega)=\sum_{m=1}^{\infty} Z_{0m}(z)[A_m(\omega)\mathrm{J}_0(\alpha_{0m}r)+B_m(\omega)\mathrm{Y}_0(\alpha_{0m}r)], \tag{16}$$

where

$$Z_{0m}(z)=\sin(k_{0m}z),\quad k_{0m}=\frac{(2m-1)\pi}{2H},\quad m=1,2,\ldots \tag{17}$$

are the acoustic modes of the volume between the cylinders in Fig. 1a and the modal wavenumbers, respectively, $\mathrm{J}_0(...)$ and $\mathrm{Y}_0(...)$ are cylindrical Bessel functions of zero order, and the radial wavenumbers α_{0m} are written as

$$\alpha_{0m}(\omega)=\sqrt{\bar{k}_0^2-k_{0m}^2}, \tag{18}$$

with acoustic wavenumber $\bar{k}_0=\omega/\bar{c}_0$ in the thorax tissue.

In the form taken, expression (16) satisfies the two-dimensional Helmholtz equation

$$\nabla^2_{(r,z)} p_0(r,z,\omega) + \bar{k}_0^2 p_0(r,z,\omega) = 0, \tag{19}$$

and the boundary conditions (4) on the lower side, $z = 0$, and upper side, $z = H$, of the outer cylinder. The unknown amplitudes $A_m(\omega)$ and $B_m(\omega)$ can be found from conditions (4) and (5) at the lateral surface of the outer cylinder, $r = R$, and the vessel surface, $r = a$, and the use of the orthogonality properties of the acoustic modes $Z_{0m}(z)$, viz.

$$\int_0^H Z_{0m}(z) Z_{0n}(z)\,\mathrm{d}z = \begin{cases} H/2 & \text{for } m = n, \\ 0 & \text{for } m \neq n. \end{cases}$$

With the coefficients $A_m(\omega)$ and $B_m(\omega)$ determined in such a manner, the expression for the random acoustic pressure $p_0(r,z,\omega)$ between the cylinders takes the form

$$p_0(r,z,\omega) = \mathrm{i}\frac{2}{H}\rho_0\omega \sum_{m=1}^{\infty} \frac{Z_{0m}(z)}{\alpha_{0m}} \frac{F(\alpha_{0m},r,R)}{G(\alpha_{0m},a,R)} \sum_{n=1}^{\infty} (-1)^{n-m} \frac{k_{vn}}{k_{vn}^2 - k_{0m}^2} V_n(\omega), \tag{20}$$

in which

$$F(\alpha_{0m},r,R) = \mathrm{J}_0(\alpha_{0m}r)\mathrm{Y}_0(\alpha_{0m}R) - \mathrm{J}_0(\alpha_{0m}R)\mathrm{Y}_0(\alpha_{0m}r),$$

$$G(\alpha_{0m},a,R) = \mathrm{J}_0(\alpha_{0m}R)\mathrm{Y}_1(\alpha_{0m}a) - \mathrm{J}_1(\alpha_{0m}a)\mathrm{Y}_0(\alpha_{0m}R)$$

are combinations of the cylindrical Bessel functions of zero and first order, and $(-1)^{n-m}k_{vn}/(k_{vn}^2 - k_{0m}^2)$ is a term that defines the degree of spatial compatibility of the acoustic, $Z_{0m}(z)$, and structural, $\Psi_{vn}(z)$, modes, viz.

$$\int_0^H Z_{0m}(z)\Psi_{vn}(z)\,\mathrm{d}z = (-1)^{n-m}\frac{k_{vn}}{k_{vn}^2 - k_{0m}^2}.$$

Substituting formula (20) into expression (15) and then into Eq. (14) yields

$$\rho_v h(\omega_{vn}^2 - \omega^2)V_n(\omega) - \rho_0\omega^2\left(\frac{2}{H}\right)^2 \sum_{q=1}^{\infty}(-1)^{n+q}V_q(\omega)\sum_{m=1}^{\infty}\frac{1}{\alpha_{0m}}\frac{F(\alpha_{0m},a,R)}{G(\alpha_{0m},a,R)}\frac{k_{vq}}{k_{vq}^2 - k_{0m}^2}\frac{k_{vn}}{k_{vn}^2 - k_{0m}^2} = \mathrm{i}\omega p_{tn}(\omega). \tag{21}$$

Making an order of magnitude analysis of Eq. (21), neglecting the terms of secondary importance and rearranging the remaining leading-order terms we obtain the approximate solution for the modal amplitudes $V_n(\omega)$, viz.

$$V_n(\omega) = \frac{\mathrm{i}\omega p_{tn}(\omega)}{a_n(\omega)}, \tag{22}$$

where

$$a_n(\omega) = \rho_v h(\omega_{vn}^2 - \omega^2) - \rho_0\omega^2\left(\frac{2}{H}\right)^2 \sum_{m=1}^{\infty}\frac{1}{\alpha_{0m}}\frac{F(\alpha_{0m},a,R)}{G(\alpha_{0m},a,R)}\frac{k_{vn}^2}{(k_{vn}^2 - k_{0m}^2)^2}. \tag{23}$$

The use of expressions (22) and (23) in formulas (13) and (20) gives one the final relationships for the vessel normal velocity, $v(z,\omega)$, and acoustic pressure, $p_0(r,z,\omega)$, respectively.

Since in the framework of the acoustic model under consideration acoustic pressure vanishes at the chest surface (see conditions (4)), the basic parameter of the sound field to be analysed at the lateral surface of the outer cylinder is the radial acceleration, w_r, viz.

$$w_r(r,z,\omega) = -\frac{1}{\rho_0}\frac{\partial p_0(r,z,\omega)}{\partial r} = \frac{2}{H}\omega^2 \sum_{m=1}^{\infty}\frac{Z_{0m}(z)}{\alpha_{0m}}\frac{\mathrm{d}F(\alpha_{0m},r,R)/\mathrm{d}r}{G(\alpha_{0m},a,R)}\sum_{n=1}^{\infty}(-1)^{n-m}\frac{k_{vn}}{k_{vn}^2 - k_{0m}^2}\frac{p_{tn}(\omega)}{a_n(\omega)}. \tag{24}$$

The spectral density $P_w(r,z,\omega)$ of the random field $w_r(r,z,\omega)$ can be obtained from the relationship of statistical orthogonality (Blake, 1986), i.e.,

$$P_w(r,z,\omega)\delta(\omega - \omega') = \langle\, w_r^*(r,z,\omega)w_r(r,z,\omega')\,\rangle, \tag{25}$$

in which the brackets $\langle ... \rangle$ denote an ensemble average, $\delta(...)$ is the Dirac delta function, and the asterisk denotes a complex conjugate. When the radial acceleration (24) is substituted into expression (25), the spectral density becomes

$$P_w(r,z,\omega) = \sum_{m=1}^{\infty}\sum_{n=1}^{\infty}(P_w(r,z,\omega))_{mn} = \left(\frac{2}{H}\omega^2\right)^2 \sum_{m=1}^{\infty}\frac{|Z_{0m}(z)|^2}{|\alpha_{0m}|^2}\frac{|\mathrm{d}F(\alpha_{0m},r,R)/\mathrm{d}r|^2}{|G(\alpha_{0m},a,R)|^2}\sum_{n=1}^{\infty}\frac{k_{vn}^2}{(k_{vn}^2-k_{0m}^2)^2}\frac{\Phi_{p_n}(\omega)}{|a_n(\omega)|^2}, \tag{26}$$

where $\Phi_{p_n}(\omega)$ are the structural modal excitation terms, defined in terms of the wavenumber–frequency spectrum of the turbulent wall pressure, $\Phi_p(k_z,\omega)$, and the shape functions of the pipe

$$|A_{vn}(k_z)|^2 = \frac{2k_{vn}^2}{(k_z^2-k_{vn}^2)^2}[1-(-1)^n\cos(k_zH)],$$

as

$$\Phi_{p_n}(\omega) = \int_{-\infty}^{\infty}|A_{vn}(k_z)|^2\Phi_p(k_z,\omega)\,\mathrm{d}k_z. \tag{27}$$

Thus, the spectral density, $P_w(r,z,\omega)$, of a radial acceleration at point (r,z) is a sum of individual mode contributions, $(P_w(r,z,\omega))_{mn}$. The modal spectral densities $(P_w(r,z,\omega))_{mn}$ are determined by the following four factors. Firstly, this is the degree of excitation of the pipe normal mode, $\Psi_{vn}(z)$, by the turbulent wall pressure which is represented in (26) by the modal excitation term $\Phi_{pn}(\omega)$. This term depends on the amplitudes of the wall pressure components and their spatial correlations with the mode $\Psi_{vn}(z)$. Secondly, this is the degree of spatial compatibility of the structural, $\Psi_{vn}(z)$, and acoustic, $Z_{0m}(z)$, modes given by the quantity $k_{vn}^2/(k_{vn}^2-k_{0m}^2)^2$. Thirdly, $(P_w(r,z,\omega))_{mn}$ is influenced by the structural response term $a_n(\omega)$ in which the resonant properties of the pipe mode $\Psi_{vn}(z)$ are reflected. Finally, these are the remaining terms in expression (26), whose combination is the transfer function of the volume between the cylinders. This function contains the geometrical characteristics of the vessel and thorax, and acoustical properties of the chest volume (such as cut-off frequencies, acoustic resonances), and describes propagation of the sound wave from the vessel to the chest surface.

All information with respect to the pipe parameters and the mean flow velocity within the pipe is mainly contained in the structural response term, $a_n(\omega)$, and the wavenumber–frequency spectrum, $\Phi_p(k_z,\omega)$, of the turbulent wall pressure, respectively, and hence, via formulas (26) and (27), in the spectrum $P_w(r,z,\omega)$. Any changes in these parameters will be reflected in the function $P_w(r,z,\omega)$. Therefore, this statistical characteristic of the random acoustic field can be used to diagnose the vessel state by changes in the field caused by vessel abnormality.

4. Analysis of the acoustic field

The analysis of the acoustic field found in the previous section is divided into the analysis of the spectrum P_w itself and the effects of variation in the pipe and flow parameters. Also the approximate dependence of the acoustic power generated by the pipe on the flow Reynolds number, $\mathrm{Re}_D = UD/\nu$, and the diameter ratio, D/d, is derived.

In calculating expression (26), the following values of the geometrical and physical parameters have been used:

$a = 1$ cm, $h = 2$ mm, $E_v = 1.35\times10^5$ N/m^2, $\rho_v = 1.15\times10^3$ kg/m^3, $\nu_v = 0.45$, $\rho = 1050$ kg/m^3, $c = 1500$ m/s, $\nu = 4\times10^{-6}$ m^2/s, $U = 0.5$–1 m/s, $R = 0.2$ m, $H = 0.4$ m, $\rho_0 = 300$ kg/m^3, $c_0 = 30$ m/s, $\mu_0 = 0.25$.

These magnitudes agree well with those cited in other papers (Borisyuk, 1998, 1999; Vovk et al., 1994a, b; Fredberg and Holford, 1983; Wang et al., 1990; Wodicka et al., 1989, 1990), and are typical for patients. The turbulent wall pressure model of Chase (1980), written for the case of one-dimensional flow, was chosen for $\Phi_p(k_z,\omega)$, viz.

$$\Phi_p(k_z,\omega) = \rho^2v_*^3[c_Mk_z^2K_M^{-5} + c_Tk_z^2K_T^{-5}], \quad K_i^2 = (\omega-U_ck_z)^2/(h_iv_*)^2 + k_z^2 + (b_i\delta)^{-2}, \quad i = M,T, \tag{28}$$

with the dimensionless coefficients $h_M \approx h_T \approx 3$, $c_T = 0.0474$, $c_M = 0.0745$, $b_T = 0.378$ and $b_M = 0.756$, recommended by Chase. This model was shown by Borisyuk (1993, 1998), Borisyuk and Grinchenko (1997) to give the best predictions of noise from low Mach number turbulence.

4.1. Acoustic power spectrum

Typical estimate of the spectrum $P_w(r,z,f)$ normalized by the quantity $(8\pi^2 f^2/H)^2 \times p_{\rm rms}^2 a/U$ is shown in Fig. 2. Here $p_{\rm rms}$ is the root-mean-square turbulent wall pressure defined as

$$p_{\rm rms} = \sqrt{\langle p_t^2 \rangle} = \sqrt{\int_{-\infty}^{\infty} P(\omega)\,{\rm d}\omega},$$

$P(\omega)$ is the wall pressure power spectrum, and $P_w(r,z,f) = 4\pi P_w(r,z,\omega)$ (Blake, 1986).

One can see that the spectrum P_w predicted within the frameworks of the acoustic model under investigation looks generally similar to the acoustic power spectrum recorded in the in vitro experiments (Borisyuk, 2000); namely, it generally decreases as the frequency increases, and exhibits local pronounced maxima.

The analysis of sound generation by the turbulence in the vessel and sound transmission from the vessel to the chest surface shows that

(i) the decrease of the function P_w with the frequency is determined mainly by both the distribution of the turbulence energy among different eddies and frequency filtering of the sound transmission due to the body tissue;

(ii) the maxima in the spectrum P_w are caused by the corresponding maxima in the functions describing in Eq. (26) the constructive elements of the acoustic model.

In fact, the influence of the turbulence on the spectrum P_w is reflected in formula (26) via the wavenumber–frequency spectrum of the turbulent wall pressure, $\Phi_p(k_z,\omega)$. A specific feature of the wavenumber–frequency spectrum (see Fig. 3a) is that, under low Mach number condition (that takes place in blood vessels), the acoustic field from turbulence is dominated by the contribution from the long-wavelength subconvective wall pressure components, $0 < k_z \ll k_c = \omega/U_c$, which are determined by the large-scale eddies (Borisyuk, 1998). These components excite the high-efficient long-wavelength structural modes Ψ_{vn} $(0 < k_{vn} \ll k_c)$ which then generate the propagating long-wavelength acoustic waves. The short-wavelength convective wall pressure components, $k_z \approx k_c$, play practically no role in producing noise by low Mach number turbulent flows. It means that the modal excitation term $\Phi_{p_n}(\omega)$ in expression (26) can be rewritten as

$$\Phi_{p_n}(\omega) \approx \int_{0<k_z\ll k_c} |A_{vn}(k_z)|^2 \Phi_p(k_z,\omega)\,{\rm d}k_z = P(\omega) \int_{0<k_z\ll k_c} |A_{vn}(k_z)|^2 \Phi_{p*}(k_z,\omega)\,{\rm d}k_z, \tag{29}$$

where $\Phi_p(k_z,\omega) = P(\omega)\Phi_{p*}(k_z,\omega)$, and $\Phi_{p*}(k_z,\omega)$ is the wavenumber–frequency spectrum normalized to unity (Blake, 1986; Borisyuk, 1993), viz.

$$\int_{-\infty}^{\infty} \Phi_{p*}(k_z,\omega)\,{\rm d}k_z = 1.$$

Representation (29) of the quantity $\Phi_{p_n}(\omega)$ indicates that the frequency content of the acoustic power, carried with the long-wavelength sound waves, is actually governed by the wall pressure power spectrum $P(\omega)$. In this spectrum (see Fig. 3b), the low-frequency domain is controlled primarily by the large-scale eddies which contain the bulk of the turbulence energy. The high-frequency domain of the function $P(\omega)$ corresponds to the small-scale vortex structures which carry a little part of the energy. As a result here the spectral level is much lower than that in the low-frequency

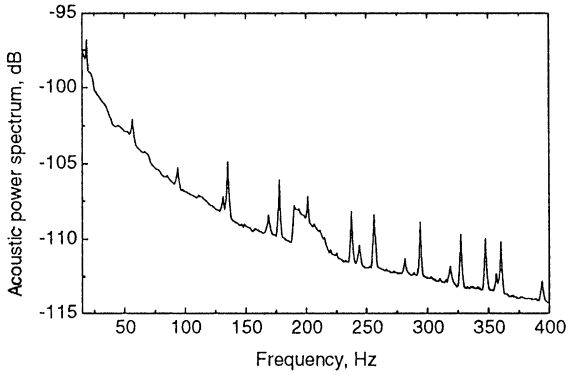

Fig. 2. Acoustic power spectrum at point $r = R$, $z = 0.5H$ generated by the conditionally normal pipe at the mean flow rate 1.27×10^{-4} m^3/s ($U = 0.5$ m/s, ${\rm Re}_D = 2250$).

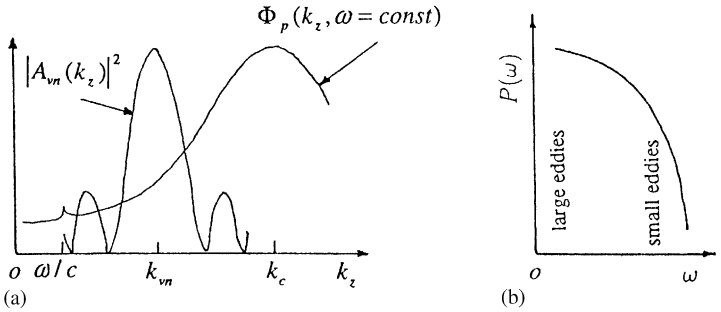

Fig. 3. (a) Wavenumber–frequency spectrum of the turbulent wall pressure, $\Phi_p(k_z, \omega)$, and shape function of the pipe, $|A_{vn}(k_z)|^2$. (b) Wall pressure power spectrum, $P(\omega)$.

Table 1
Resonance frequencies of the pipe

Mode number	1	2	—	10	—	15	—	20	—	30	—
Frequency, Hz	193.15	193.1502	—	193.27	—	193.76	—	195.1	—	202.84	—

Table 2
Acoustic resonances

Resonance number	1	2	3	4	5	6	7	8	9	—
Frequency, Hz	134.3	177.5	200.9	237.5	256.2	293.7	327.5	347.5	360.8	—

range, the level decreasing rapidly with frequency (it corresponds to the decrease in the vortex energy with the decrease of its size).

Such distribution of the turbulence energy among the eddies results in that the main part of the acoustic energy radiated by the vibrating vessel travels with the low-frequency long-wavelength sound waves. The other sound waves contain much less acoustic energy, the energy decreasing with frequency.

In travelling from the vessel to the chest surface, the sound waves undergo the influence of the body tissue, which is reflected in the transfer function in expression (26). The tissue has been shown by Vovk et al. (1994a) to act as a low-frequency filter. In other words, the body allows propagation of the low-frequency content and filters off the high-frequency content of the sound field. As a result the low-frequency sound waves reach the chest surface, whereas the high-frequency waves have much difficulties and lose much energy in reaching the body surface. This explains the general decrease of the sound level with frequency at the chest surface, as shown in Fig. 2.

The maxima in the spectrum P_w observable in Fig. 2 result from the corresponding maxima in the functions representing in Eq. (26) the constructive elements of the acoustic model under investigation. Firstly, these are the peaks at the resonance frequencies of the vibrating pipe (Table 1) which are contained in the structural response term, $a_n(\omega)$. Secondly, the acoustic resonances of the chest volume (they are reflected in the quantity G of the transfer function) produce the corresponding peaks in the spectrum P_w at the frequencies given in Table 2. Finally, the maxima at the frequencies presented in Table 3 correspond to the cut-off frequencies of the body volume, $\omega_m = c_0 k_{0m}$. These maxima appear in the transfer function when the wavenumber α_{0m} reaches the minimum.

4.2. Effects of the pipe parameters

4.2.1. Effects of the wall thickness

The influence of the wall thickening Δh on the acoustic power spectrum can be seen from Fig. 4 where the spectra produced by two pipes of different wall thickness at the same mean flow rate, $U\pi D^2/4 = u\pi d^2/4$, are presented. The comparison of the curves shows that the sound levels from the thickened pipe of *mild* severity $S = 14\%$, quantified as

$$S = [1 - (d/D)^2] \times 100\% \approx \Delta h/a \times 100\%, \tag{30}$$

Table 3
Cut-off frequencies

Frequency number	1	2	3	4	5	6
Frequency, Hz	18.75	56.25	93.75	131.25	168.75	206.25
Frequency number	7	8	9	10	11	—
Frequency, Hz	243.75	281.25	318.75	356.25	393.75	—

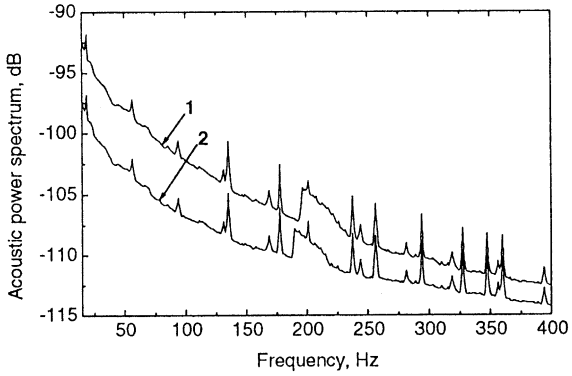

Fig. 4. Acoustic power spectra at point $r = R$, $z = 0.5H$ generated by two pipes of different wall thickness at the mean flow rate 1.27×10^{-4} m^3/s ($U = 0.5$ m/s, $\mathrm{Re}_D = 2250$); $1 - h + \Delta h = 3.4$ mm, $S = 14\%$; $2 - h = 2$ mm.

are noticeably higher than those from the conditionally normal pipe, the difference between the levels generally decreasing as the frequency increases. Also there is the difference between the location of the maxima in curves 1 and 2 in the frequency band 190 Hz$<f<$230 Hz (these maxima are associated with the pipe resonances at the frequencies ω_{vn}). The location of the other peaks (corresponding to the cut-off frequencies and the acoustic resonances of the chest volume) does not change in transiting from curve 2 to curve 1.

The same modification of the acoustic power spectrum due to thickening of the pipe wall (i.e., nonuniform growth of the level and the displacement of the maxima at the frequencies ω_{vn}) was obtained also for the other estimates of expression (26). This indicates that thickening of the vessel wall is associated with the *two basic* acoustic effects. These are a general increase in the sound level and the shift (to the right) of the peaks at the vessel natural frequencies in the acoustic power spectrum. The latter effect can be treated as the production of new frequency components.

The first effect is explained by that, under the mass conservation condition (7), increase in the wall thickness causes both an increase in the local flow energy (i.e., from the value of order ρU^2 in the conditionally normal pipe to ρu^2 in the partially constricted pipe) and redistribution of the energy among the appropriate flow scales (i.e., mainly from the large eddies of sizes of order $D/2$ moving at speeds of order U in the normal pipe to the large vortices of dimensions of order $d/2$ which are convected at speeds of order u in the narrowed pipe). This leads to the higher amplitudes of the turbulent wall pressure p_t, and hence the higher levels of the wall pressure spectra $P(\omega)$ and $\Phi_p(k_z, \omega)$ (the changes in the power spectrum $P(\omega)$ are herewith such that the spectrum level grows mainly in the low-frequency domain determinable by the large vortex structures; see Fig. 5). Such variations in the noise source structure then are reflected in the modal excitation term (29), and, via Eq. (26), result in the corresponding nonuniform increase of the sound level, as shown in Fig. 4.

The second effect of wall thickening is due to the corresponding increase in the pipe resonance frequencies (12) and the subsequent displacement (to the right) of the maxima at ω_{vn} in the spectrum P_w.

The other peaks in the function P_w are attributed to the cut-off frequencies and the acoustic resonances of the body. The body properties are insensitive to the changes in the vessel parameters. Consequently, variations in the vessel thickness do not influence these two groups of the frequencies, and hence the location of the corresponding maxima in the spectrum P_w.

4.2.2. Effects of the physical parameters of the pipe wall

Variations in Young's modulus of the pipe wall, E_v, result in the corresponding variations in both the bending stiffness, D_v, and the resonance frequencies, ω_{vn}. The fluid flow and the turbulent wall pressure p_t do not change

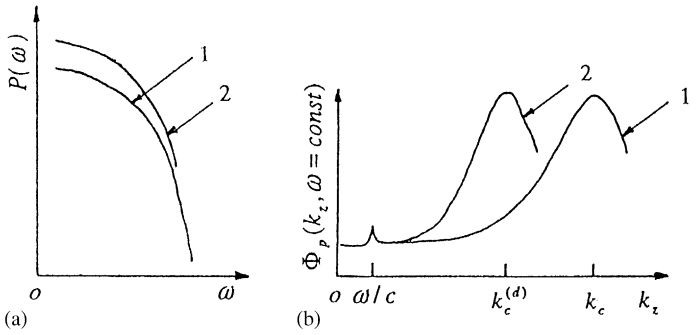

Fig. 5. Power spectrum (a) and wavenumber–frequency spectrum (b) of the turbulent wall pressure in conditionally normal (curve 1) and thickened (curve 2) pipes.

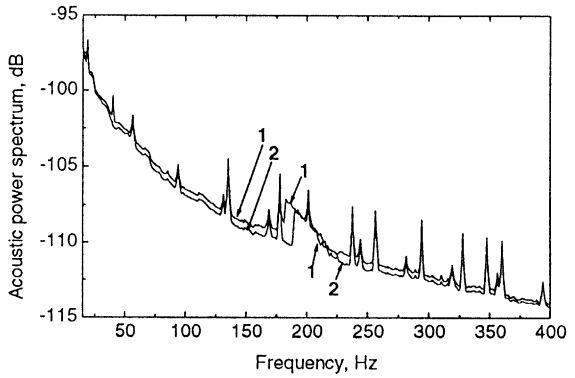

Fig. 6. Acoustic power spectra at point $r = R$, $z = 0.5H$ generated at the mean flow rate 1.27×10^{-4} m^3/s ($U = 0.5$ m/s, $\mathrm{Re}_D = 2250$); $1 - E_v = 1.2 \times 10^5$ N/m^2; $2 - E_v = 1.35 \times 10^5$ N/m^2.

herewith within the framework of the acoustic model under investigation. In such situation, the sound levels and the positions of the maxima in the spectrum P_w must change in the appropriate way, namely, increase in the value of E_v must cause, on the one hand, the increase in the bending stiffness D_v, and hence, under the invariable exciting force p_t, the decrease in both the amplitude of the pipe vibration and sound levels radiated. On the other hand, resonance frequencies (12) must increase, which result in the shift (to the right) of the maxima at the frequencies ω_{vn} in the spectrum P_w.

Decrease in the modulus of elasticity must cause an increase of the sound levels and displacement (to the left) of the peaks at the frequencies ω_{vn}.

This is demonstrated in Fig. 6 where the acoustic power spectra from two pipes having the different values of Young's modulus are depicted. The comparison of the curves shows that the small increase/decrease in E_v causes the small decrease/increase of the sound levels generated and the shift (to the right/left) of the maxima at the natural frequencies ω_{vn} in the range 180 Hz$<f<$210 Hz. The other maxima correspond to the cut-off frequencies and the acoustic resonances of the body volume, and therefore their position is insensitive to the variations in the Young's modulus.

Similar changes in the spectrum P_w result from the variations in Poisson's ratio ν_v (Fig. 7). A small decrease/increase in the quantity ν_v is seen to cause a small increase/decrease of the sound levels and the displacement (to the left/right) of the peaks at the natural frequencies ω_{vn} in the range 180 Hz$<f<$210 Hz.

A small decrease/increase in the mass density of the pipe wall, ρ_v, is associated with a shift (to the right/left) of the maxima at the frequencies ω_{vn} in the range 190 Hz$<f<$230 Hz and a small increase/decrease of the acoustic power levels (Fig. 8).

The explanation of the effects found in Figs. 7 and 8 is similar to the Young's modulus effects.

The above cases of separate variations in the vessel parameters are, in principle, possible but not very realistic. More realistic are situations when appearance of a stenosis is associated with simultaneous changes either in all the

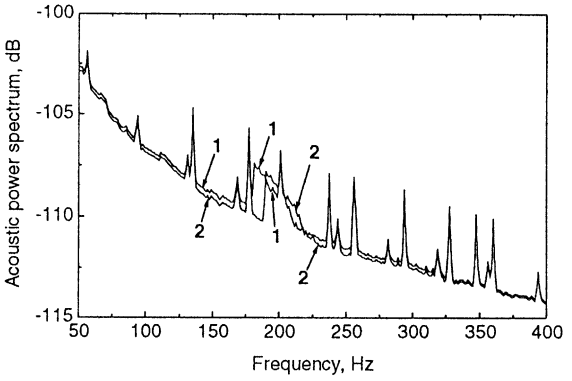

Fig. 7. Acoustic power spectra at point $r = R$, $z = 0.5H$ generated at the mean flow rate 1.27×10^{-4} m^3/s ($U = 0.5$ m/s, $\mathrm{Re}_D = 2250$); $1 - \nu_v = 0.3$; $2 - \nu_v = 0.45$.

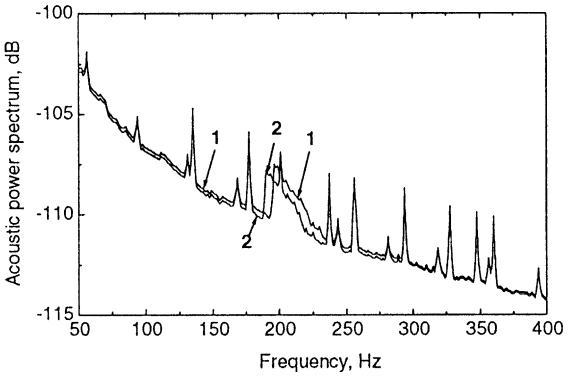

Fig. 8. Acoustic power spectra at point $r = R$, $z = 0.5H$ generated at the mean flow rate 1.27×10^{-4} m^3/s ($U = 0.5$ m/s, $\mathrm{Re}_D = 2250$); $1 - \rho_v = 1.05 \times 10^3$ kg/m^3; $2 - \rho_v = 1.15 \times 10^3$ kg/m^3.

parameters considered or in some of them (including the wall thickness h). In this case, the modifications in the spectrum P_w will evidently be the combination of the modifications found above.

4.3. Mean flow velocity effects

It is well known in medical practice (Mirolyubov, 1983; Young, 1979) that the difference between the noise levels from the stenosed and originally healthy vessels (which is one of the basic parameters to be analysed in diagnosing the vessel state) depends on flow rate. This results in that, under resting flow conditions (the patient rests), the difference can be so small that rather strong stenosis cannot be detected. However, under elevated flow conditions (manual labour), the difference increases, and the stenosis becomes detectable. It is interesting to see whether this effect can be predicted within the frameworks of the acoustic model under investigation.

For this purpose, the noise spectra from the conditionally normal pipe and from the pipe having the other value of one of the wall parameters were calculated for the different mean flow velocities and compared. One can see from Figs. 4 and 9 that the difference between the sound levels from the thickened and normal pipes increases with U and vice versa, the decrease in U results in the reduction of the difference.

Such changes in the difference between the sound levels with the mean flow velocity correlate qualitatively well with those noted above. The explanation of this velocity effect is similar to the explanation of the effects found in Section 4.2. It is based on the analysis of variations of the appropriate terms in expression (26) with U, made for the cases of normal and thickened pipes.

Variations in the physical parameters of the pipe wall were said in Section 4.2 not to influence the fluid flow. Consequently, the flow is identical within the conditionally normal pipe and the pipe having the other value of some physical parameter. In such a situation, the changes in the mean flow velocity will equally influence the sound fields

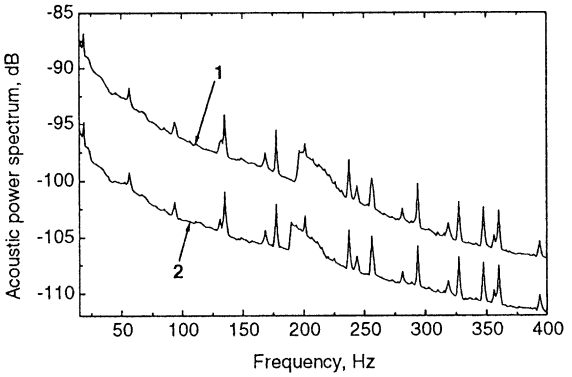

Fig. 9. Acoustic power spectra at point $r = R$, $z = 0.5H$ generated by two pipes of different wall thickness at the mean flow rate 2.03×10^{-4} m^3/s ($U = 0.8$ m/s, $\mathrm{Re}_D = 3600$); $1 - h + \Delta h = 3.4$ mm, $S = 14\%$; $2 - h = 2$ mm.

from the pipes. As a result, there will be no changes in the difference between the sound levels from the pipes with U, as was obtained in the appropriate calculations of this study.

4.4. Dependence of the acoustic power on Re_D and D/d

The modifications in the spectrum P_w with the pipe thickness and the mean flow velocity were demonstrated in Sections 4.2.1 and 4.3, respectively. It was shown that, apart from the other effects, a mild increase in the wall thickness and/or the mean flow velocity causes an increase in both the acoustic power level and a difference between the levels from the thickened and conditionally normal pipes. Those data were, however, of a qualitative character. In order to know how much the indicated parameters influence the sound field, it is necessary to have the corresponding quantitative estimates.

Some of these estimates can be obtained from the following arguments. The pressure fluctuations in the pipe flow are directly proportional to the fluid mass density and the second power of the mean flow velocity (Blake, 1986). This gives for the thickened pipe:

$$p_t \sim \rho u^2,$$

or taking into account formula (8), this expression becomes

$$p_t \sim \rho U^2 (D/d)^4 \approx \rho U^2 \left(1 + \frac{\Delta h}{2a}\right)^4.$$

The normal velocity of the vessel wall, v, and the acoustic pressure in the thorax, p_0, can be written as

$$v = p_t \times T_v, \quad p_0 = v \times T_b = p_t \times T_v T_b,$$

where T_v and T_b are the functions reflecting the vessel and thorax properties, respectively.

The acoustic power produced by the vibrating vessel, Π, then can be written as

$$\Pi \sim p_0^2 \sim \rho^2 U^4 (D/d)^8 \times T_v^2 T_b^2 \approx \rho^2 U^4 \left(1 + \frac{\Delta h}{2a}\right)^8 \times T_v^2 T_b^2.$$

Introducing the fluid viscosity, ν, in this relationship gives

$$\Pi \sim (\mathrm{Re}_D)^4 (D/d)^8 \times \frac{\rho^2 \nu^4}{D^4} T_v^2 T_b^2 \approx (\mathrm{Re}_D)^4 \left(1 + \frac{\Delta h}{2a}\right)^8 \times \frac{\rho^2 \nu^4}{D^4} T_v^2 T_b^2.$$

For a given pipe, fluid and acoustic medium between the pipe and the cylinder, the magnitude $\rho^2 \nu^4 T_v^2 T_b^2 / D^4$ is constant and therefore,

$$\Pi \sim (\mathrm{Re}_D)^4 (D/d)^8 \approx (\mathrm{Re}_D)^4 \left(1 + \frac{\Delta h}{2a}\right)^8. \tag{31}$$

This relationship agrees reasonably well with that obtained experimentally by Borisyuk (2000), and indicates that the acoustic power from a slightly thickened pipe is approximately proportional to the fourth power of the flow Reynolds number in the originally normal pipe and the eighth power of the ratio of the pipe diameters.

Using similar arguments, it is easy to show that the difference in the acoustic power produced by thickened and originally normal vessels, $\Delta\Pi$, is

$$\Delta\Pi \sim (\mathrm{Re}_D)^4[(D/d)^8 - 1]. \tag{32}$$

The difference is seen to increase as the flow Reynolds number, Re_D, and/or the diameter ratio, D/d, increase. This correlates well with the appropriate effects of the mean flow velocity and wall thickness found in Sections 4.3 and 4.2.1, respectively.

Writing the ratio of the acoustic powers from two thickened vessels of differing severities, Π_1 and Π_2, we have

$$\frac{\Pi_1}{\Pi_2} \sim \frac{d_2^8}{d_1^8}.$$

This relationship indicates that an approximately 30% decrease in the vessel diameter (i.e., $d_2/d_1 \approx 1.33$) causes a 10-fold increase in the radiated acoustic power (one order of magnitude).

5. Conclusions

An acoustic generation of noise by a larger human blood vessel and noise transmission in the thorax have been modelled and studied in this work. In doing this, the random statistical nature of the noise sources, the basic vessel properties and the main features of the human chest structure have been taken into account. Also the effects of changes in the basic vessel parameters have been considered as a first attempt to study acoustic effects of a vascular stenosis. The corresponding results obtained and their analysis allow one to make the following conclusions.

1. In the framework of the proposed acoustic model of noise generation and transmission, a relationship (26) has been obtained. It relates the acoustic power spectrum in the body to the vessel and flow parameters, and also reflects the influence of the human thorax on the acoustic field.

2. Predictions for the acoustic power spectrum, made for the typical vessel and flow conditions, show that the spectrum looks generally similar to the acoustic power spectrum observable in in vitro studies.

3. Mild thickening of the vessel wall causes noticeable increase in the sound level and a shift (to the right) of the peaks at the vessel resonance frequencies in the acoustic power spectrum.

Small increase/decrease in Young's modulus of the vessel wall results in a small decrease/increase in the sound level and a displacement (to the right/left) of the maxima at the vessel natural frequencies in the acoustic power spectrum. Similar changes in the spectrum are caused by small variations either in Poisson's ratio or the mass density of the vessel wall.

Variations in the acoustic power spectrum caused by simultaneous changes either in all the vessel parameters considered or in some of them will be the combination of the variations noted above.

4. The acoustic power generated by a slightly thickened (deseased) vessel is approximately proportional to the fourth power of the flow Reynolds number in the originally normal (healthy) vessel and the eighth power of the ratio of the vessel diameters (see expression (31)).

The difference in the sound power from the vessels increases as the diameter ratio and/or the flow Reynolds number increase, as given by formula (32).

5. An approximately 30% decrease in the vessel diameter causes a 10-fold increase in the radiated acoustic power (one order of magnitude).

6. The proposed acoustic model is only a first step in modelling noise generation by a larger human blood vessel and noise transmission in the body. The model is based on rather general assumptions and, therefore, the results obtained and the corresponding conclusions made in this study are essentially qualitative. Other investigations of the fluid loading in arterial blood flow, as well as research into the properties of vessels and the human chest are necessary in order to improve the model.

Acknowledgements

The author gratefully acknowledges the financial support of the Alexander von Humboldt Foundation (Germany).

References

Blake, W.K., 1986. Mechanics of Flow-Induced Sound and Vibration, Vols. 1,2. Academic Press, New York.

Borisyuk, A.O., 1993. Vibration and sound radiation by elastic plates excited by turbulent flow. Ph.D. Dissertation, Institute of Hydromechanics, Kiev, Ukraine (in Russian).

Borisyuk, A.O., 1998. Modeling of the acoustic properties of a larger human blood vessel. Acoustic Bulletin 1 (3), 3–13.

Borisyuk, A.O., 1999. Noise field in the human chest due to turbulent flow in a larger blood vessel. Flow, Turbulence and Combustion 61, 269–284.

Borisyuk, A.A., 2000. Modeling of noise generation by a vascular stenosis. Acoustic Bulletin 3 (2), 3–18 (in Russian).

Borisyuk, A.O., Grinchenko, V.T., 1997. Vibration and noise generation by elastic elements excited by a turbulent flow. Journal of Sound and Vibration 204, 213–237.

Chase, D.M., 1980. Modeling the wavevector–frequency spectrum of turbulent boundary layer wall pressure. Journal of Sound and Vibration 70, 29–67.

Corcos, G.M., 1963. The resolution of pressure in turbulence. Journal of the Acoustical Society of America 35, 192–199.

Duncan, G.W., Gruber, J.O., Dewey Jr., C.F., Myers, G.S., Lees, R.S., 1975. Evaluation of carotid stenosis by phonoangiography. New England Journal of Medicine 293, 1124–1128.

Fredberg, J.J., 1974. Pseudo-sound generation at atherosclerotic constrictions in arteries. Bulletin of Mathematical Biology 36, 143–155.

Fredberg, J.J., 1977. Origin and character of vascular murmurs: model studies. Journal of the Acoustical Society of America 61, 1077–1085.

Fredberg, J.J., Holford, S.K., 1983. Discrete lung sounds: crackles (rales) as stress-relaxation quadrupoles. Journal of the Acoustical Society of America 73, 1036–1046.

Junger, M.S., Feit, D., 1972. Sound, Structures and their Interaction. MIT Press, Cambridge, MA.

Lees, R.S., Dewey Jr., C.F., 1970. Phonoangiography: a new noninvasive diagnostic method for studying arterial disease. Proceedings of the National Academy of Sciences USA 67, 935–942.

Martin, N.C., Leehey, P., 1977. Low wavenumber wall pressure measurements using a rectangular membrane as a spatial filter. Journal of Sound and Vibration 52, 95–120.

Mirolyubov, S.G., 1983. Hydrodynamics of stenosis. Modern Problems in Biomechanics 1, 73–136 (in Russian).

Vovk, I.V., Grinchenko, V.T., Krasnyi, L.G., Makarenkov, A.P., 1994a. Breath sounds: recording and classification problems. Akusticheskii Zhurnal 40, 50–56 (in Russian).

Vovk, I.V., Zalutskii, K.E., Krasnyi, L.G., 1994b. Acoustic model of the human respiratory system. Akusticheskii Zhurnal 40, 762–767 (in Russian).

Wang, J., Tie, B., Welkowitz, W., Semmlow, J.L., Kostis, L.B., 1990. Modeling sound generation in stenosed coronary arteries. IEEE Transactions of Biomedical Engineering 37, 1087–1094.

Wodicka, G.R., Stevens, K.N., Golub, H.L., Growalho, E.G., Shanon, D.C., 1989. A model of acoustic transmission in the respiratory system. IEEE Transactions of Biomedical Engineering 36, 925–933.

Wodicka, G.R., Stevens, K.N., Golub, H.L., Shanon, D.C., 1990. Spectral characteristics of sound transmission in the human respiratory system. IEEE Transactions of Biomedical Engineering 37, 1130–1134.

Young, D.F., 1979. Fluid mechanics of arterial stenoses. Journal of Biomechanical Engineering 101, 157–175.